Pressure-induced phase matching in high-order harmonic generation

S. Kazamias,[1,2] S. Daboussi,[1,2] O. Guilbaud,[1,2] K. Cassou,[1,2] D. Ros,[1,2] B. Cros,[1] and G. Maynard[1]

[1]*Laboratoire de Physique des Gaz et des Plasmas, CNRS - Université Paris-Sud 11, F-91405 Orsay Cedex, France*
[2]*LASERIX-CLUPS-Université Paris-Sud 11, F-91405 Orsay Cedex, France*

We present an alternative explanation of the high-order-harmonic-generation experimental results published recently by Seres *et al.* [Nature Phys. **6**, 455 (2010)]. We show that the physical interpretation can be comprehensively done in the frame of classical theory of high-order harmonic generation without referring to a parametric effect in the XUV domain. The experimental conditions explored by Seres *et al.* indeed correspond to the case of long-pulse, low-infrared-energy laser beams for which tight focusing is necessary to reach the minimum intensity required for high atomic response. The positive atomic dispersion can compensate for the Gouy phase and explains the behavior of the experimental variation of the harmonic signal presented. We will show that our interpretation explains not only the global behavior of the curves but also the second-order variation of the signal as a function of experimental parameters.

PACS number(s): 32.80.Qk, 32.30.Jc

I. INTRODUCTION

Due to its wide field of application, high-order harmonic source obtained from the interaction between an intense laser pulse and a rare gas has been extensively studied for the last 20 years. Since the first experimental demonstration at the end of the 1980s [1], the conversion efficiency has considerably progressed from about 10^{-9} [1] in 1990, to 10^{-8} in 1993 [2], 10^{-7} in 1995 [3], and 5×10^{-6} in 1998 [4]; the evolution in time is exponential until 2000 with 10^{-5} [5]. These advances were due to a better theoretical understanding of both the atomic response [6] and the phase-matching conditions [7,8]. Meanwhile, development and technical progress on high-energy short-pulse-duration [9] laser systems have been done. The most efficient high-order harmonic generation takes place in experimental conditions where the focusing is quite loose, the pressure relatively low, and the laser intensity quite high [10,11].

Historically, the use of low pump energy, long-pulse-duration lasers was progressively withdrawn because it required quite tight focusing and the conversion efficiency was lower than for loose focusing. The high-order harmonic generation in those conditions had not been extensively studied for several years. Recently published experimental results [12] provide a wide range of new data obtained in those conditions with high dynamics detectors. We will show that classical phase-matching analysis can provide a physical interpretation of what is observed experimentally [13]. We analyze more specifically the influence of gas pressure, harmonic order, maximum laser intensity, and focusing conditions on high-order harmonic generation. The quite low conversion efficiency obtained by Seres *et al.* [12] of near 10^{-7} is also compatible with our analysis.

II. OVERVIEW OF THE BASIC THEORY OF HIGH-ORDER HARMONICS

High-order harmonic generation (HHG) is a highly nonlinear process induced in rare gases by an intense laser field with ultrashort pulse duration: in the picosecond or femtosecond regime. The intensity reached at focus, of the order of

10^{14} W/cm^2, is so high that the laser field is comparable to the electric field between the core and the electron. Twice in an optical cycle, tunnel ionization can occur; afterward the quasifree electron is accelerated in the laser electric field. If the laser polarization is strictly linear, there can be a recollision between the electron and the parent ion when the electric field changes sign. During the radiative recombination, a harmonic photon is produced with an energy corresponding to the sum of the kinetic energy acquired in the laser field and the ionization potential of the atom. This three-step model was first analyzed in 1992 [14,15] using a semiclassical approach and afterward through a full quantum understanding in 1994 in the frame of the strong field approximation (SFA) [6]. This model allows the quantitative prediction of both harmonic dipole phase and amplitude as a function of the laser intensity. It explains the quantum origin of the two quantum paths with their different phases connected to the time spent in the continuum by the electron before it recollides with its parent ion.

The macroscopic growth of the harmonic signal along the propagation in the generative medium is the result of phase-matching considerations. For a given order q, the instantaneous harmonic signal $S_{\mathrm{HHG}}(t)$ at the output of a medium with length l_{med} depends on the coherence length l_{coh} and on the absorption length l_{abs} following the law [16]

$$S_{\mathrm{HHG}}(t) \propto \frac{4 l_{\mathrm{abs}}^2 P^2 A_q(t)^2}{1 + 4\pi^2 \left[l_{\mathrm{abs}}^2 / l_{\mathrm{coh}}(t)^2 \right]} \times \left[1 + e^{-\frac{l_{\mathrm{med}}}{l_{\mathrm{abs}}}} - 2\cos\left(\pi \frac{l_{\mathrm{med}}}{l_{\mathrm{coh}}(t)} \right) e^{-\frac{l_{\mathrm{med}}}{2 l_{\mathrm{abs}}}} \right], \quad (1)$$

where P is the gas pressure and A_q is the individual harmonic dipole amplitude. Following the results presented by Lewenstein [6], A_q strongly depends on time through its variation with laser intensity. The laser intensity is compared with I_{cutoff}, the minimum intensity required for a given harmonic to be efficiently generated. If $I > I_{\mathrm{cutoff}}$ then A_q scales as $\left(\frac{I}{I_{\mathrm{cutoff}}}\right)^{4.6}$, otherwise it is taken as $\left(\frac{I}{I_{\mathrm{cutoff}}}\right)^{10.6}$, which means logically almost zero [17]. The second dependence of A_q comes from the fact that only nonionized atoms are considered for harmonic generation: A_q thus scales with the proportion of neutral atoms.

Lengths l_{med} and l_{abs} are constant in time, but the coherence length can rapidly change within the infrared pulse duration because of the ionization process that influences the electronic and atomic dispersions. It is given by $l_{coh} = \frac{\pi}{|\delta k|}$, where the wave-vector mismatch δk between infrared and XUV fields is (the notation is the same as for Ref. [5]):

$$\delta k = q(\delta k_{at} + \delta k_{elec} + \delta k_{Gouy}) + \delta k_{\phi_{at}}, \qquad (2)$$

where δk_{Gouy} is known as the Gouy phase gradient and depends on laser focusing conditions, and $\delta k_{\phi_{at}}$ is the atomic phase gradient and depends on the quantum path. Within the pulse duration, the maximum harmonic emission is obtained as a compromise between phase-matching considerations and atomic response. High atomic response would require high laser intensity but at the same time high intensity generates a high ionization level that damages phase matching. Phase matching is reached when the coherence length is greater than the medium length so that no destructive interferences of the coherent signal can occur between two harmonic dipoles with π phase difference [16]. The absorption limit is obtained when the medium length is also longer than a few times the absorption length. When absorption-limited generation is reached, the two other ways of still increasing the signal is to increase the laser intensity at which the perfect phase matching occurs [5] or increase the transverse dimension of the beam [10,11,18]: this is the so-called loose focusing technique obtained when the Rayleigh range is much longer than the medium length.

III. DESCRIPTION OF THE 1D MODEL

A one-dimensional (1D) numerical code, described in detail in Ref. [5], has been written to analyze the high-order harmonic generation. This code was adapted to study the case of low intensity, tight focusing, and high gas pressure recently published in Fig. 2 of Ref. [12].

The harmonic signal from H31 to H55 was calculated using the same parameters as in [12]: argon gas pressure up to 2 bars, laser intensity of $(1–5) \times 10^{14}$ W/cm^2, temporal Gaussian envelope with duration up to 350 fs, 1050-nm wavelength, $z_0 = 5$ mm Rayleigh range, medium length $l_{med} = 2$ mm, and medium entrance located at $z_{cell} = 2$ mm from the laser focal position.

Table I presents the absorption lengths (in mm) for argon for harmonic 31 to harmonic 55 for a pressure of 100 mbar [19]. Note also that it scales inversely with pressure.

The atomic dispersion for a 1050-nm laser wavelength in argon is given by

$$\delta k_{at}[\text{mm}^{-1}] = 1.66 \times 10^{-3} \times P[\text{mbar}](1 - \tau), \qquad (3)$$

where τ is the ionization degree calculated from the Ammosov, Delone and Krainov rates [20] and solving the differential system of atomic and argon ion species.

Electronic dispersion depends on the infrared laser wavelength according to the plasma dispersion law:

$$\delta k_{elec} = \frac{\omega}{c}\delta n_{elec} = -\frac{\omega}{c}\frac{n_e}{2n_c}, \qquad (4)$$

with

$$n_e = \frac{\tau P}{k_B T}, \qquad (5)$$

and

$$n_c = \frac{\omega^2 m_e}{\mu_0 c^2 e^2}, \qquad (6)$$

$$\delta k_{elec}[\text{mm}^{-1}] = -\frac{\lambda P[\text{mbar}](0.1\tau\mu_0 e^2)}{4\pi m_e k_B T}. \qquad (7)$$

For $\lambda = 1050$ nm it is given by

$$\delta k_{elec}[\text{mm}^{-1}] = -0.07366 \times \tau P[\text{mbar}], \qquad (8)$$

The atomic phase gradient plays a role in phase matching; the corresponding wave-vector mismatch is expressed for both the first and the second quantum paths using

$$\delta k_{\phi_{at}} = -\alpha \nabla I, \qquad (9)$$

with $\alpha = 2 \times 10^{-14}$ cm^2/W for the first quantum path and $\alpha = 22 \times 10^{-14}$ cm^2/W for the second one [21].

The calculation of the time dependence of the above wave-vector mismatches allows us to determine the value of $l_{coh}(t)$ and then the instantaneous value of the harmonic flux from Eq. (1). The total harmonic signal is integrated over the whole pulse duration separately for quantum paths 1 and 2, then the total signal is summed for both contributions [21].

IV. RESULTS OBTAINED FROM THE 1D CODE

Figures 1 and 2 present in semilogarithmic scale the time-integrated harmonic signals for H31 and H55, respectively, as a function of the gas pressure for different laser intensities.

The laser intensities are 1, 1.5, and 2 $\times 10^{14}$ W/cm^2. For the sake of comparison, the curve marked with $*$ corresponds to a quadratic growth. As a first conclusion, the theoretical predictions obtained using a 1D model are in qualitative agreement with the experimental data in [12]. Figures 1 and 2 clearly exhibit the harmonic signal increase over four orders of magnitude at low pressures below 100 mbar observed experimentally. Furthermore, they reproduce the two different behaviors observed at high pressures in [12]: signal saturation for high intensities and decrease for low intensities. An important point is that the saturation of the signal with pressure starts almost for the same pressure for all the harmonic orders, which shows that this effect is not due to

TABLE I. Absorption lengths (in mm) in argon for harmonic 31 to harmonic 55 and a pressure of 100 mbar.

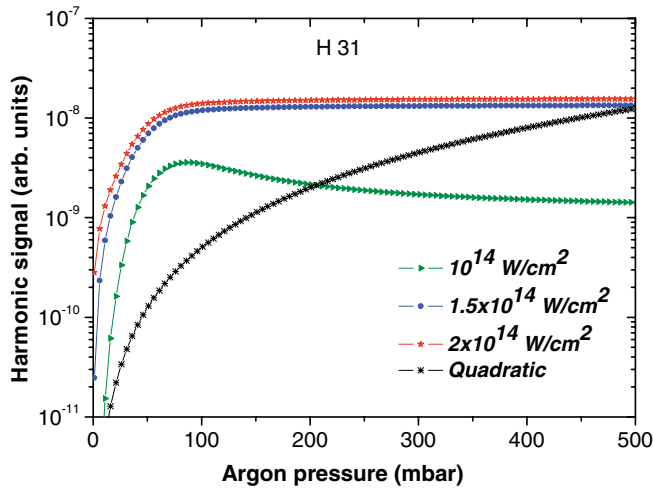| Order	31	33	35	37	39	41	43	45	47	49	51	53	55
l_{abs}	0.23	0.60	1.34	2.72	4.03	4.45	4.65	4.49	4.25	3.98	3.68	3.40	3.18

FIG. 1. (Color online) Signal from H31 in argon as a function of pressure for three laser intensities. A pure quadratic law is also indicated.

culated as a function of pressure for a 1050-nm pump wavelength:

$$l_{\mathrm{coh}}(\tau = 0) \approx \frac{\pi/q}{|\delta k_{\mathrm{Gouy}} + \delta k_{\mathrm{at}}|}$$

$$\approx \frac{\pi/q}{\left| \frac{1}{z_0 + z_{\mathrm{cell}}^2/z_0} - P \times 1.66 \times 10^{-3} \right|}$$

$$\approx 600 \frac{\pi/q}{|P_{\mathrm{opt}} - P|}. \qquad (10)$$

l_{coh} increases up to the optimum pressure for which the atomic dispersion exactly compensates the Gouy phase gradient. The coherence length becomes theoretically infinite for

$$P_{\mathrm{opt}} = \frac{600}{z_0 + \frac{z_{\mathrm{cell}}^2}{z_0}}. \qquad (11)$$

This optimum pressure is obviously independent of the harmonic order q, but inversely scales with the Rayleigh range: the shorter the focusing, the greater the effect. For the lowest intensity (10^{14} W/cm^2), thus low ionization ($\tau \sim 0$), Fig. 2 shows the evolution of l_{coh} of H31 as a function of pressure for $z_0 = 5$ mm and $z_{\mathrm{cell}} = 2$ mm.

When the gas remains neutral during the whole infrared pulse duration, the coherence length remains constant in time and the maximum of the harmonic emission occurs at the maximum of the infrared laser intensity. The signal can be analytically calculated as a function of gas pressure by including Eq. (10) into Eq. (1). The result is presented in Fig. 3 together with a pure quadratic law. We conclude that the fast growth of the high-order harmonic signal at low pressures is explained by the coherence length increase with pressure in addition to the quadratic growth of the atomic response with gas density [the P^2 term in Eq. (1)]. Note that this is valid for any harmonic order, because P_{opt} is independent of q. The signal decrease after the maximum is also due to the coherence length decrease with pressure after the maximum value. These results compare well with Fig. 2(b) of Ref. [12]. Note that the experimental conditions, not only the high quality
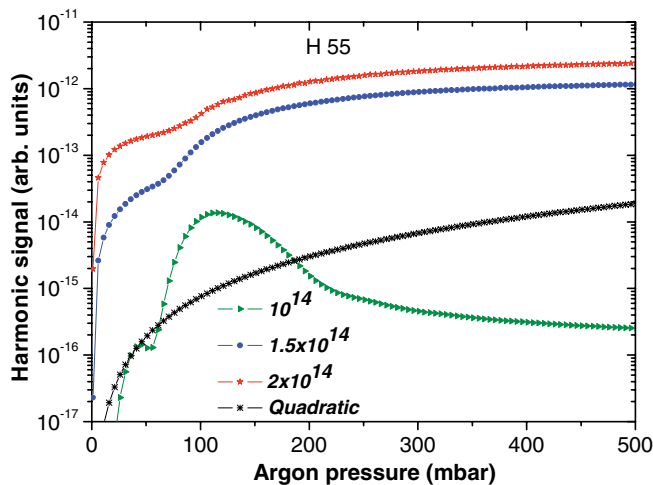
reabsorption, since absorption strongly depends on harmonic order (see Table I). The 1D simulations also reproduce the curve inflexion, the so-called shoulder, observed only for a high-order harmonic (H55) at low intensity for a pressure around 100 mbar (see Fig. 2(a) of Ref. [12]). The explanation of these characteristics in the following paragraphs, including second-order effects such as the shoulders, will show that our model provides an accurate understanding of the high-order-harmonic-generation processes involved in the experiment.

V. DEPENDENCE OF THE COHERENCE LENGTH WITH THE PRESSURE AT LOW INTENSITY

At low laser intensity, i.e., when the ionization rate in the medium and the atomic phase gradient can be neglected, the coherence length can be analytically cal-

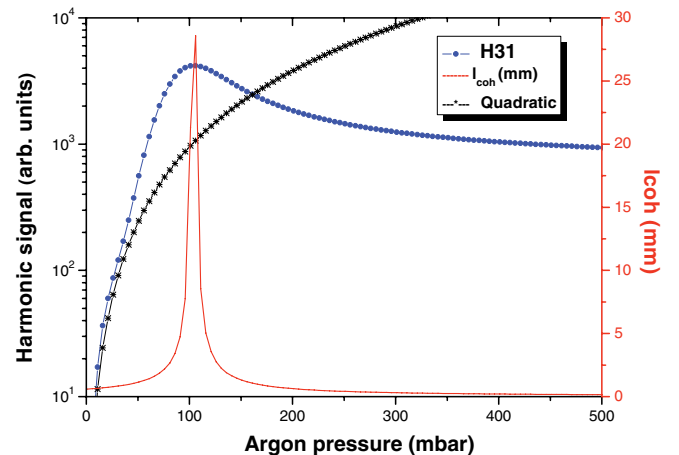FIG. 2. (Color online) Same as Fig. 1, but for the signal from H55 in argon.

FIG. 3. (Color online) Analytical H31 signal as a function of pressure (○) as compared to pure quadratic increase (∗), the coherence length evolution (in mm) is shown in full line.

of the experimental setup but also the broad detection range of Ref. [12], were very appropriate to seeing this strong increase in coherence length with pressure, which was predicted as early as 1999 [7].

This simple time-independent view only works for low intensities. At higher laser intensity in order to get higher harmonic orders, the ionization level in the medium at the maximum of the laser pulse can reach a few percents (for 350-fs pulse duration, 10^{14} W/cm^2 leads to 1% whereas 2×10^{14} W/cm^2 leads to 80%). The phase-matching behavior is then more complicated and connected to temporal effects as we will see in the following.

VI. PHASE-MATCHING OPTIMIZATION IN PRESENCE OF IONIZATION

A. Position of the problem

It is well known that the production of an efficient atomic response for a high-order harmonic requires high laser intensity as this is a highly nonlinear effect. Moreover a minimum laser intensity is needed for a given harmonic to be efficiently generated [15]. This laser intensity, called I_{cutoff}, increases with the harmonic order and also corresponds to some ionization degree in the medium, especially for long pulse duration as in Ref. [12] (where the laser pulse duration is 350 fs).

At a given ionization degree τ and considering only the first quantum path for which the atomic phase is almost zero, the coherence length becomes

$$
\begin{aligned}
l_{\text{coh}}(\tau) &\approx \frac{\pi/q}{|\delta k_{\text{Gouy}} + \delta k_{\text{at}} + \delta k_{\text{elec}}|} \\
&\approx \frac{\pi/q}{\left| \frac{1}{z_0 + \frac{z_{\text{cell}}^2}{z_0}} - 10^{-3} P (1.66 - 73.66 \times \tau) \right|} \\
&\approx 600 \frac{\pi/q}{|P_{\text{opt}}(0) - P(1 - 44\tau)|}.
\end{aligned}
\tag{12}
$$

The pressure that leads to the highest coherence length is now given by

$$
P_{\text{opt}}(\tau) = \frac{600}{\left(z_0 + \frac{z_{\text{cell}}^2}{z_0} \right)(1 - 44\tau)}.
\tag{13}
$$

The ionization rate reduces the positive effect of atomic dispersion. As long as $\tau < 2\%$, the above phase-matching analysis is still valid except that the value of P_{opt} is increased following Eq. (13). For τ larger than $\approx 2\%$, P_{opt} becomes negative and the atomic dispersion is no longer able to compensate for the Gouy phase mismatch at the maximum of the pulse. In the following we will study the consequence of this, in the cases of high and low pressures.

B. Behavior for pressures higher than the optimum

For pressures largely above the optimum, the sign of the total δk in Eqs. (2) and (12) changes and the value of l_{coh} is dominated by the dispersive term that becomes much larger than the Gouy phase mismatch. If the laser intensity is high enough, an amount of ionization close to $\tau = 2\%$ optimizes
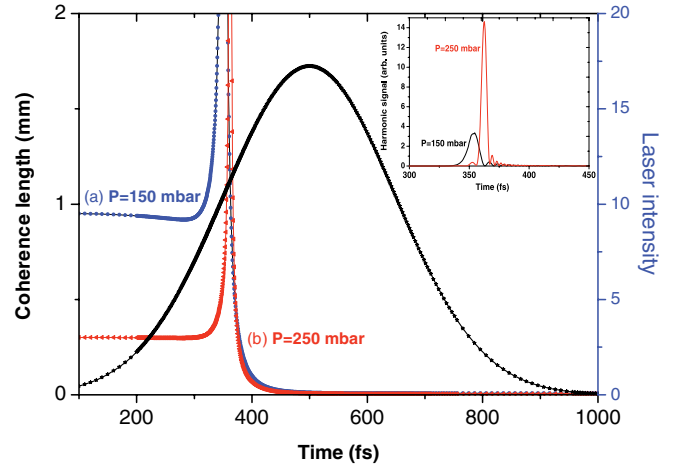

FIG. 4. (Color online) H43 temporal evolution of both the coherence length in mm and the harmonic signal in arbitrary units for pressures of 150 and 250 mbar. The unlabeled curve represents the infrared laser envelope, $I = 2.10^{14}$ W/cm^2.

the coherence length since the τ for which l_{coh} is infinite is equal to $\frac{1}{44}(1 - \frac{P_{\text{opt}}(0)}{P})$. This amount increases with P up to the $\tau = 2\%$ limit and explains why the curves at high intensity and high pressure from Fig. 2 in Ref. [12] do not decrease and even still increase slowly: the higher the pressure, the higher the laser intensity at which perfect phase matching occurs. An illustration of this is provided in Fig. 4 which shows both the temporal evolution of the coherence length and the H43 harmonic signal at two different pressures above the optimum one, i.e., 150 and 250 mbar, and $I = 2 \times 10^{14}$ W/cm^2. This effect of course cannot take place at low intensities for which τ remains zero all along the pulse and l_{coh} decreases as $1/P$ $[P > P_{\text{opt}}(0)]$.

C. Behavior for pressures lower than the optimum

If the pressure is too low, that is, lower than $P_{\text{opt}}(0)$, there is no value of ionization for which the infinite coherence length can be reached. Moreover the coherence length decreases with τ. Efficient harmonic generation then occurs at the beginning of the rising front of the pulse for which τ is as low as possible. In that case, high laser intensity is not compatible with good phase matching.

This was observed at a fixed laser intensity by comparing different harmonic orders: in Fig. 2(b) of Ref. [12] the exponential slope of the signal is much larger for a low-order harmonic such as H31, which requires only a low intensity to be generated, than for a much higher-order harmonic such as H43.

Another consequence is that the signal increase with the laser intensity for a given harmonic will be small. A striking illustration of this is the absolute calibration of the harmonic signal for H31 in Fig. 2 from Ref. [12]: whereas the optimized signal in pressure reaches 0.5 nJ per pulse at 1.1×10^{14} W/cm^2 and even 2 nJ for 1.5×10^{14} W/cm^2, it falls down to 6×10^{-2} nJ at 4×10^{14} W/cm^2.

The above analysis clearly shows why the atomic dispersion compensation of the Gouy phase mismatch is appropriate for low-intensity lasers and quite tight focusing. When phase

matching at high intensity is desired, the only way to reach it is to reduce the Gouy phase mismatch, which is the principle of the "loose focusing" phase matching. As explained more in detail in Refs. [5,18], when the Gouy phase mismatch becomes almost negligible, phase matching is reached when the atomic and electronic dispersions compensate for each other: that corresponds to a precise ionization rate (here $\tau = 2\%$) but is independent of gas pressure.

VII. DESTRUCTIVE INTERFERENCE BETWEEN THE HARMONIC DIPOLES: ORIGIN OF THE SHOULDERS

A. Low-intensity case

As can be observed around 100 mbar in Fig. 1 for H55, the harmonic signal growth presents a slight inflexion of the curve arising, which we call the shoulder in the following. This is also observed experimentally in the results presented in Fig. 2 from Ref. [12]. These shoulders occur for a large number of harmonic orders, and are much more pronounced at low intensities. It can be explained by destructive interference within the medium between harmonic dipoles exactly separated by l_{coh} [22]. This is clearly visible in the cosine term in Eq. (1). When increasing the pressure, the coherence length increases [Eq. (10)] but reaches some values for which the medium length exactly corresponds to even multiples of it: this is mainly given by $l_{coh} = 1$ mm in the experimental case for which $l_{med} = 2$ mm. The signal then stops its rapid growth with pressure until the pressure increase allows the coherence length to be far from this destructive value. Equation (6) shows that the $1/q$ dependence of l_{coh} with harmonic order predicts a slightly higher pressure for higher q to reach 1 mm. This effect is clearly visible on the data in Fig. 2(a) of Ref. [12].

B. High-intensity case

When the intensity is higher, the time dependence of the coherence length plays a key role but the interpretation in terms of destructive interference is still the same. As can be seen in Fig. 5, which shows both the coherence length and harmonic signal evolution in time for three pressures around the shoulder, the value of the coherence length before ionization is higher than 1 mm, but through the ionization process (in our case the intensity reaches 10^{14} W/cm^2 and $\tau = 1.2\%$), it goes through this destructive value during the laser pulse. The most negative effect will occur when the 1 mm value is reached at the maximum of the pulse, case (b) for which the pressure is 85 mbar.

Looking at Eq. (12), it is then easy to understand why the shoulder occurs for higher pressures at higher intensities, since the value of the coherence length must be larger than one at the beginning of the pulse. This is clearly visible in Fig. 2 of Ref. [12]: shoulders occur around 0.1 bar for $I = 1.5 \times 10^{14}$ W/cm^2 and are close to 0.2 bar for $I = 1.5 \times 10^{14}$ W/cm^2.

At even higher intensities and higher pressures, the shoulder effect almost disappears since fringes are blurred by time integration: the coherence length reaches destructive values too fast or too often in the pulse.
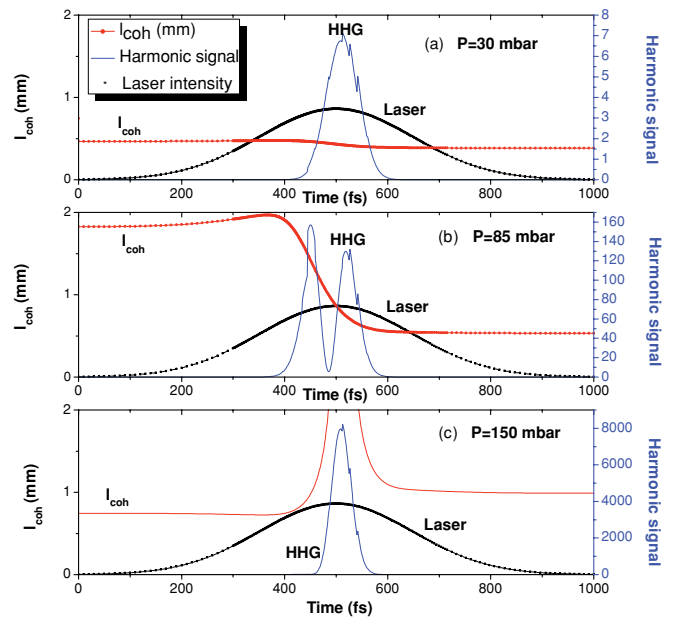

FIG. 5. (Color online) H55 temporal evolution of both the coherence length in mm (circles) and the harmonic signal in arbitrary units (triangles) for three pressures. The black curve represents the infrared laser envelope, $I = 10^{14}$ W/cm^2.

VIII. CONCLUSION

Using a analytical 1D time-dependent model of high-order harmonic generation, we have explained the interplaying roles of gas pressure, focusing geometry, and laser intensity on phase matching in a range of parameters relevant to recent experimental observations [12] in argon. Without any adjustable parameter, our model reproduces the more than quadratic growth of the harmonic signal with pressure. Moreover, we explain as a function of harmonic order and laser intensity the different ways the curves saturate, which was not even mentioned nor numerically reproduced by Seres *et al.* [12]. Our model shows the origin of curve inflexion at low pressures and how it behaves with harmonic order and laser intensity, the x-ray parametric amplification model proposed by Seres does not.

Our 1D model is unable to quantitatively predict the harmonic spectra and spatial distribution. However, a hypothesis can be proposed to explain the experimental results described in [12]. A very low divergence beam plus reduced spectral width were observed for the high level of harmonic signal at optimum pressure, whereas they were both large for the low level signal. This case corresponds to what the authors call a seed beam and which is harmonic generation at too low of a pressure. We think this difference can be explained in terms of the transition between phase matching from the first to the second quantum path [22,23]. It has indeed been well known since 1995 [24] that the second quantum path leads to a larger divergence and a much larger spectrum than the first one, both on the blue and the red sides [25], through the atomic phase derivative in time.

Concerning the specific case of helium, and despite the low atomic dispersion of this gas, our model also predicts a rapid increase of the signal with pressure at the beginning of the curve, but it fails to explain the position of the maximum for

the different harmonic orders. Our interpretation is that three-dimensional effects such as strong beam defocusing are occurring, since the laser intensity is as high as 2×10^{16} W/cm^2. A more refined code with the time-dependent Schrödinger equation (TDSE) and three-dimensional propagation of the laser in a strongly ionized medium would probably be able to reproduce the experimental curves.

An important point concerning the experimental results from Ref. [12] is whether or not they provide a signature of self-stimulated harmonic emission as mentioned by Seres *et al.* Our conclusion based on the very good agreement between our model and the experimental data is that any self-stimulated contribution is negligible in the experimental conditions of [12].

[1] L. A. Lompré, A. L'Huillier, M. Ferray, P. Monot, G. Mainfray, and C. Manus, J. Opt. Soc. Am. B **7**, 754 (1990).

[2] Anne L'Huillier and Ph. Balcou, Phys. Rev. Lett. **70**, 774 (1993).

[3] T. Ditmire, J. K. Crane, H. Nguyen, L. B. DaSilva, and M. D. Perry, Phys. Rev. A **51**, R902 (1995).

[4] S. G. Preston, D. M. Chambers, R. S. Marjoribanks, P. A. Norreys, D. Neely, M. Zepf, J. Zhang, M. H. Key, and J. S. Wark, J. Phys. B **31**, 1069 (1998).

[5] S. Kazamias, D. Douillet, F. Weihe, C. Valentin, A. Rousse, S. Sebban, G. Grillon, F. Augé, D. Hulin, and Ph. Balcou, Phys. Rev. Lett. **90**, 193901 (2003).

[6] M. Lewenstein, Ph. Balcou, M. Yu. Ivanov, A. L'Huillier, and P. B. Corkum, Phys. Rev. A **49**, 2117 (1994).

[7] C. G. Durfee, A. R. Rundquist, S. Backus, C. Herne, M. M. Murnane, and H. C. Kapteyn, Phys. Rev. Lett. **83**, 2187 (1999).

[8] A. Rundquist, C. G. Durfee, Z. Chang, C. Herne, S. Backus, M. M. Murnane, and H. C. Kapteyn, Science **29**, 1412 (1998).

[9] M. Schnürer, Z. Cheng, M. Hentschel, G. Tempea, P. Kálmán, T. Brabec, and F. Krausz, Phys. Rev. Lett. **83**, 722 (1999).

[10] J.-F. Hergott, M. Kovacev, H. Merdji, C. Hubert, Y. Mairesse, E. Jean, P. Breger, P. Agostini, B. Carré, and P. Salieres, Phys. Rev. A **66**, 021801(R) (2002).

[11] Y. Tamaki, J. Itatani, M. Obara, and K. Midorikawa, Phys. Rev. A **62**, 063802(R) (2002).

[12] J. Seres, E. Seres, D. Hochhaus, B. Ecker, D. Zimmer, V. Bagnoud, T. Kuehl, and C. Spielmann, Nature Phys. **6**, 455 (2010).

[13] S. Kazamias, S. Daboussi, O. Guilbaud, K. Cassou, C. Montet, O. Neveu, D. Ros, B. Cros, and G. Maynard, Nature Phys. **6**, 927 (2010).

[14] P. B. Corkum, Phys. Rev. Lett. **71**, 1994 (1993).

[15] J. L. Krause, K. J. Schafer, and K. C. Kulander, Phys. Rev. Lett. **68**, 3535 (1992).

[16] E. Constant, D. Garzella, P. Breger, E. Mevel, Ch. Dorrer, C. Le Blanc, F. Salin, and P. Agostini, Phys. Rev. Lett. **82**, 1668 (1999).

[17] This value was discussed with Philippe Balcou in 2001 and comes from the analysis of Figs. 3 and 4 in [6].

[18] S. Kazamias, F. Weihe, D. Douillet, C. Valentin, T. Planchon, S. Sebban, G. Grillon, F. Augé, D. Hulin, and Ph. Balcou, Eur. Phys. J. D **21**, 353 (2002).

[19] The Center for X-Ray Optics website: [www.cxro.lbl.gov].

[20] N. P. Delone and V. P. Krainov, Phys. Usp. **41**, 469 (1998).

[21] Ph. Balcou, A. S. Dederichs, M. B. Gaarde, and A. L'Huillier, J. Phys. B **32**, 2973 (1999).

[22] S. Kazamias, D. Douillet, C. Valentin, F. Weihe, F. Augé, Th. Lefrou, G. Grillon, S. Sebban, and Ph. Balcou, Phys. Rev. A **68**, 033819 (2003).

[23] Ph. Balcou, P. Salières, A. L'Huillier, and M. Lewenstein, Phys. Rev. A **55**, 3204 (1997).

[24] P. Salieres, A. L'Huillier, and M. Lewenstein, Phys. Rev. Lett. **74**, 3776 (1995).

[25] D. H. Reitze *et al.*, Opt. Lett. **29**, 86 (2004).